

Interaction of linear waves and moving Josephson vortex lattices in layered superconductors

A. V. Chiginev* and V. V. Kurin

Institute for Physics of Microstructure of the Russian Academy of Science, GSP-105, 603950 Nizhny Novgorod, Russia

(Dated: May 13, 2017)

A general phenomenological theory describing dynamics of Josephson vortices coupled to wide class of linear waves in layered high- T_c superconductors is developed. The theory is based on hydrodynamic long wave approximation and describes interaction of vortices with electromagnetic, electronic and phonon degrees of freedom on an equal footing. In the limiting cases the proposed theory degenerates to simple models considered earlier. In the framework of the suggested model we undertook the numerical simulation of resistive state in layered superconductors placed in external magnetic field and demonstrate excitation of linear waves of various origin by a moving vortex lattice, manifesting in existence of resonances on current-voltage characteristics.

I. INTRODUCTION

High- T_c superconductors (HTSCs) with strong anisotropy has been the subject of intensive investigation during many years. The layered structure, intrinsic Josephson effect, and complex chemical composition provide a variety of physical properties of such materials. A great deal of attention has been paid to Josephson dynamics of layered superconductors.

The application of an external magnetic field parallel to the layers to a layered HTSC leads to formation of a Josephson vortex lattice (JVL) which can be moved under the influence of an external current applied perpendicular to the layers. When this lattice collides with the edge of the structure the electromagnetic radiation is generated. This principle may be used for construction of small and efficient electromagnetic oscillators with the frequency being limited from above by the energy gap in HTSC which is of the order of 10 THz. Recently, the radiation with the frequency of 0.85 THz and power of $0.5 \mu\text{W}$ has been obtained from the structure based on $\text{Bi}_2\text{Sr}_2\text{CaCu}_2\text{O}_8$ ¹. The small and compact sources of electromagnetic radiation of terahertz band are very interesting for applications in astrophysics, medicine, biology and many other branches of science. Therefore, the investigation of Josephson dynamics in layered HTSCs is highly important.

Layered HTSCs represent complex physical system with wide spectrum of eigenwaves, which includes electromagnetic, plasma, different phonon modes and Carlson-Goldman mode². All these modes are coupled to vortices and can be excited by the moving JVL. The reverse action of the excited waves on JVL resulting in changes of vortex shape and mutual arrangement of vortices will affect the current-voltage characteristics (CVCs) of layered superconductor and intensity of electromagnetic radiation. Thus coupling of linear modes and moving vortices can be practically used for controlling the dispersion properties of eigenwaves by the external magnetic field, for diagnostics of eigenwaves by methods of Josephson spectroscopy³, and for controlling electromagnetic radiation from layered superconductor.

The model adequately describing vortex dynamics in layered HTSCs should take into account the interaction of vortices with all weakly damping linear modes. However, the development of the theory of such comprehensive kind is not a simple task and a main obstacle is a nonlocality of the constitutive equations of a layered superconductor or, in other words, spatial dispersion. Even in hydrodynamic approximation when the dynamical equations are differential, the consistent approach to description of layered media requires solution of differential equations for field and matter in the domains of homogeneity, and subsequent joining of the solutions found for adjacent domains on interfaces. If the number of modes in the system is rather high then the exact description leads to sophisticated problem for eigenvectors and eigenvalues of high-dimension transfer matrix. Example of calculations of this kind applied to normal nonsuperconducting layered media can be found in Ref. 4. The description of layered systems can be considerably simplified by employing the long-wavelength limit which deals with smoothed dynamical variables averaged over the spatial period of the layered structure. The goal of the present paper is the development of such a theory for a layered superconductor with intrinsic Josephson effect. We propose an averaged, sufficiently simple, hydrodynamic theory accounting for a wide spectrum of linear waves and vortex degrees of freedom. The model is easily extendable for including additional linear modes and mechanisms of their excitation.

By present, a number of models describing Josephson dynamics of layered HTSCs in some special cases has been proposed. The first and most known one is the local model accounting only for the magnetic (inductive) coupling between adjacent junctions of the stack which was applied to description of the artificial multilayer Josephson structures⁵ and later to layered superconductors with intrinsic Josephson effect⁶. The charge coupling between the adjacent junctions in layered superconductors has first been investigated in Ref. 7 for the case of spatially uniform distributions of Josephson phase. There have been also some attempts to combine magnetic and charge couplings into one model^{8,9}.

The "global" coupling of the junctions via the external waveguide connected parallel to the long Josephson junction stack has been considered in our previous paper¹⁰. The influence of nonequilibrium effects, such as quasiparticle imbalance, to the Josephson dynamics of intrinsic junctions in layered HTSCs, has been investigated in Refs. 11–14. The effects of the in-plane dissipation to the Josephson vortex motion in layered HTSCs has been studied in Refs. 15–17. The role of phonons in Josephson dynamics has been considered in Refs. 18,19 for the case of direct excitation of phonons by the electric field, in Refs. 20,21 for phonon excitation due to phonon-assisted tunneling. All these models may be unified into one theory describing the linear waves and Josephson vortices in layered HTSCs.

In the present paper we formulate the comprehensive theory accounting for vortex interaction with linear waves of different physical nature which unifies the models mentioned above. The prescription to design a theory of such kind is the following. Instead of exact consideration of high- T_c superconductor as a layered medium we consider it as a continuous anisotropic medium which consists of superconducting and normal electrons and of several sort of ions. To describe the dynamics of such a media coupled to electromagnetic field we use Maxwell equations jointly with two-liquid anisotropic hydrodynamic equations for electrons and equations of adiabatic Born-Oppenheimer approximation for ions. But this set of equations describe only linear properties of layered superconductor in long-wave limit. To introduce vortex degrees of freedom to the model and allow finite jump of Josephson phase difference on dielectric layers we "discretize" the set of equations simultaneously restoring the nonlinear term with sinusoidal dependence on Josephson phase difference in interlayer current. In various particular cases our model is reduced to the known models considered earlier. In the framework of the suggested model we undertook the numerical simulation of resistive state in layered superconductors placed in external magnetic field and demonstrate excitation of linear waves of various origin by a moving vortex lattice, manifesting in existence of resonances on current-voltage characteristics.

The paper is organized as follows. The next section is devoted to formulation of effective averaged model describing linear waves and vortex degrees of freedom in layered superconductors with intrinsic Josephson effect and to estimation of effective parameters of the model. The third section is devoted to numerical experiment showing the effects of excitation of linear waves by Josephson vortex lattice moving in a layered HTSC. In the conclusion we summarize the main results obtained in the paper.

II. THE PHENOMENOLOGICAL DESCRIPTION OF JOSEPHSON DYNAMICS OF A LAYERED HTSC — HYDRODYNAMIC APPROACH.

In this section we derive the set of equations describing Josephson dynamics of a layered superconductor treating it as a continuous but anisotropic medium. First, we write down the Maxwell equations and anisotropic hydrodynamic equations describing superconducting condensate, electronic quasiparticles and phonon degrees of freedom of superconductor. As a result of this stage we obtain a system describing linear waves in a layered HTSC in a long wavelength limit. Then, substituting the derivatives over the coordinate perpendicular to the layers by finite differences and, simultaneously, restoring the nonlinear expression for the interlayer supercurrent in Josephson form $j_s = j_c \sin \theta_n$, we obtain the desired set of equations.

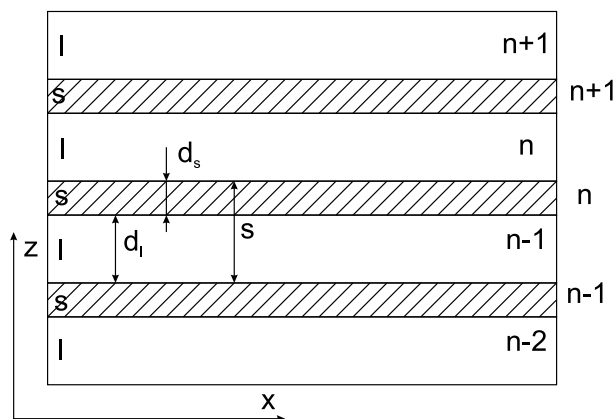


FIG. 1: Side view of the multilayer Josephson structure. The numeration of superconducting and insulator layers, and the coordinate system, are shown.

In this paper we adopt the widely used concept that high- T_c superconductor can be treated as a sequence of superconducting layers coupled through dielectric layers by tunnel effect providing the existence of Josephson effect and quasiparticle conductivity in c -axis direction. Such a layered superconductor with chosen coordinate system is

shown in Fig. 1. The x axis is chosen laying in ab plane of a superconductor which is assumed to be isotropic in this plane, direction of the y axis is chosen coinciding with the direction of the magnetic field which is assumed to have only one component, both static and alternating, and the z axis is directed perpendicular to the layers along c axis of layered superconductor. For such magnetic field the electric field and other physical variables would not depend on y and the problem becomes two-dimensional one. The superconducting and adjacent dielectric layers are enumerated by number n , as shown in Fig. 1.

We start the derivation from the assumption that, first, the characteristic scale of the solutions is much greater than the layer structure period, and, second, the module of the Josephson phase difference over dielectric layer is much smaller than unity. These assumptions allow us to treat layered superconductor as a continuous medium, and, thus, to formulate the desired model in the continual limit. Then, after "discretizing" the continuous model, we will restore possibility of finite jump of the phase of the order parameter and finally obtain the set of finite-difference equations representing the desired model allowing vortex solutions.

As the basic equations we use Maxwell equations for electromagnetic field together with hydrodynamic equations describing contributions from superconducting electrons, normal electrons, and phonons. The next subsections are devoted to derivation of constitutive equations needed to construct the desired model.

A. Field equations and superconducting electrons

In this subsection we derive the set of equations phenomenologically describing Josephson dynamics of a layered superconductor in a continual limit. To do this, first we use Maxwell equations together with anisotropic hydrodynamic equations for superconducting electrons. Afterwards we supplement the set of obtained equations with constitutive equations describing contributions from normal electrons and phonons, which are to be derived in the next subsections.

As the starting point of the derivation of the equations describing the superconducting electron subsystem we use the expression of the superconducting momentum which we denote as \mathbf{p} via the phase χ of superconducting order parameter

$$\mathbf{p} = \hbar \nabla \chi + \frac{2e}{c} \mathbf{A}, \quad (1)$$

here \mathbf{A} is the vector potential of the electromagnetic field and the negative electron charge is explicitly taken into account. On this stage we suppose that there are no vortices in the material, so that $[\nabla \times \nabla \chi] = 0$. Accounting for this, we obtain

$$\mathbf{B} = \frac{c}{2e} [\nabla \times \mathbf{p}]. \quad (2)$$

Substituting this expression into Maxwell equation $[\nabla \times \mathbf{B}] = 4\pi c^{-1} \mathbf{j}_{tot} + c^{-1} \dot{\mathbf{E}}$ we get the evolutional equation for \mathbf{E}

$$\frac{1}{c} \dot{\mathbf{E}} = \frac{c}{2e} [\nabla \times [\nabla \times \mathbf{p}]] - \frac{4\pi}{c} \mathbf{j}_{tot}. \quad (3)$$

The total current \mathbf{j}_{tot} in (3) is the sum of the supercurrent \mathbf{j}_s , current of normal electrons \mathbf{j}_n , and ion current \mathbf{j}_i . The supercurrent is related to velocity by usual expression $\mathbf{j}_s = -en_0\mathbf{v}$ but in anisotropic Ginzburg-Landau model the momentum is connected to velocity by relation $\mathbf{p} = 2\hat{m}_s\mathbf{v}$ via tensor \hat{m}_s of effective mass. We write down this tensor in the form $\hat{m}_s = \text{diag}(m/\Gamma_s, m\Gamma_s)$, where $m = (m_{xx}m_{zz})^{1/2}$ is the geometric average of the effective masses of superconducting electrons in the in-plane and interlayer directions, factor $\Gamma_s = (m_{xx}/m_{zz})^{1/2}$ is a measure of anisotropy of superconducting properties of the material. Using the expression for supercurrent, one rewrites (3) in components

$$\frac{1}{c} \dot{E}_x = \frac{c}{2e} \left(\frac{\partial^2 p_z}{\partial x \partial z} - \frac{\partial^2 p_x}{\partial z^2} \right) - \frac{4\pi}{c} \left(-\frac{en_0\Gamma_s}{2m} p_x + j_{n_x} + j_{i_x} \right), \quad (4a)$$

$$\frac{1}{c} \dot{E}_z = \frac{c}{2e} \left(-\frac{\partial^2 p_z}{\partial x^2} + \frac{\partial^2 p_x}{\partial x \partial z} \right) - \frac{4\pi}{c} \left(-\frac{en_0}{2m\Gamma_s} p_z + j_{n_z} + j_{i_z} - j_{ext} \right). \quad (4b)$$

Though we assume that nothing depends on y -coordinate in our system, in the Eq. (4b) we take into account that the z -component of $[\nabla \times \mathbf{B}]$ actually consists of two terms

$$[\nabla \times \mathbf{B}] = \frac{\partial B_y}{\partial x} - \frac{\partial B_x}{\partial y} \equiv \frac{\partial B_y}{\partial x} + \frac{4\pi}{c} j_{ext};$$

with the last term in the r. h. s. of this equation being proportional to the bias current j_{ext} . The Eqs. (4a), (4b) are to be supplemented with evolutionary equations for \mathbf{p} .

If we differentiate Eq. (1) with respect to time and introduce chemical potential of superconducting electrons $2\mu = \hbar\dot{\chi} - 2e\varphi$ then we come to equation of hydrodynamic type

$$\hat{m}\dot{\mathbf{v}} + \nabla\mu = -e\mathbf{E}. \quad (5)$$

Further we make a model assumption that chemical potential of superconducting electrons is defined by formula of degenerated Fermi gas $\mu = \varepsilon_F$ where $\varepsilon_F = \hbar^2(3\pi^2n)^{2/3}/2m$ is the Fermi energy and n is a concentration of superconducting electrons. Assuming that deviation of the concentration n_s from its equilibrium value n_0 is small we can linearize equation (5) what yields

$$\hat{m}_s\dot{\mathbf{v}}_s + \frac{2}{3}\varepsilon_{F,s}\frac{n_s}{n_0} = -e\mathbf{E}, \quad (6)$$

where we denote as $\varepsilon_{F,s} = \varepsilon_F(n = n_0)$ a Fermi energy for unperturbed superconducting concentration. Further, excluding the concentration deviation n_s from hydrodynamic equations using Maxwell equation which we write in the form $(\nabla \cdot \mathbf{D}) = 4\pi\rho_s \equiv -4\pi en_s$, we come to evolutionary equation for \mathbf{p}

$$\frac{1}{2e}\dot{\mathbf{p}} = \mathbf{E} - r_d^2\nabla(\nabla \cdot \mathbf{D}), \quad (7)$$

or, in components

$$-\frac{1}{2e}\dot{p}_x = E_x - r_d^2\left(\frac{\partial^2 D_x}{\partial x^2} + \frac{\partial^2 D_z}{\partial x\partial z}\right), \quad (8a)$$

$$-\frac{1}{2e}\dot{p}_z = E_z - r_d^2\left(\frac{\partial^2 D_x}{\partial x\partial z} + \frac{\partial^2 D_z}{\partial z^2}\right). \quad (8b)$$

Here $r_d = (2/3)^{1/2}v_F/\omega_p$ is a screening length of longitudinal electric field, $v_F^2 = 2\varepsilon_F/m$, and $\omega_p^2 = 4\pi e^2 n_0 m^{-1}$ are averaged Fermi velocity and plasma frequency respectively which are defined as $v_F^2 = (v_{F_x}^2 v_{F_z}^2)^{1/2}$, $\omega_p^2 = (\omega_{p_x}^2 \omega_{p_z}^2)^{1/2}$. Vector of electric displacement field \mathbf{D} is defined so that it includes charges of normal electrons and ions as bound charges, i.e.

$$\mathbf{D} = \mathbf{E} + 4\pi\mathbf{P}_n + 4\pi\mathbf{P}_i \equiv (\hat{I} + 4\pi\hat{\chi}_n + 4\pi\hat{\chi}_i)\mathbf{E}, \quad (9)$$

where \mathbf{P}_n and \mathbf{P}_i are the polarizations associated with normal electrons and phonons, respectively, so that $(\nabla \cdot \mathbf{P}_{n,i}) = -\rho_{n,i}$. Tensors $\hat{\chi}_n$, $\hat{\chi}_i$ are normal electrons and phonons susceptibility respectively.

A set of equations Eqs. (4a), (4b), (8a), (8b) describes linear dynamics of electromagnetic field and superconducting condensate in layered superconductor in the long wave limit. Other degrees of freedom as normal quasiparticles and phonons of different kind come in the Eqs (4a), (4b) via extra current densities \mathbf{j}_n , \mathbf{j}_i and in the Eqs. (8a), (8b) via displacement vector \mathbf{D} . In the next two subsection we find contributions from quasiparticles and phonons to susceptibility and make the set of equations complete.

B. Contribution from normal electrons

To describe normal electrons we assume that they form degenerate Fermi gas and apply hydrodynamical Thomas-Fermi approach what gives the following equations

$$\begin{aligned} \dot{n}_n + n_{0n}(\nabla \cdot \mathbf{v}_n) &= 0, \\ \hat{m}_n(\dot{\mathbf{v}}_n + \hat{\nu}\mathbf{v}_n) + \frac{2}{3}\frac{\varepsilon_F}{n_{0n}}\nabla n_n &= e\mathbf{E}. \end{aligned} \quad (10)$$

In the Eqs. (10) $\hat{m}_n = \text{diag}(m/\Gamma_n, m\Gamma_n)$ is the mass tensor of normal electrons, Γ_n is the anisotropy parameter, n_{0n} is the unperturbed electron concentration, n_n is the deviation of electron concentration from its unperturbed value, \mathbf{v}_n is the electron velocity, $\varepsilon_{F,n} = \varepsilon_F(n = n_{0,n})$ is the Fermi energy of normal electrons and tensor $\hat{\nu} = \text{diag}(\nu_x, \nu_z)$ characterizes the electron collision frequencies. For superconductor the condition $\omega \ll \nu_{x,z}$ is usually satisfied and equations can be somewhat simplified by neglecting the term $\dot{\mathbf{v}}$ in comparison with $\hat{\nu}\mathbf{v}$. Then such hydrodynamic

equations can be solved and the relation between normal current \mathbf{j}_n and electric field \mathbf{E} can be easily obtained. In (ω, \mathbf{k}) -representation one gets

$$\mathbf{j}_n = \frac{\omega_{pn}^2}{4\pi\Delta} \begin{pmatrix} 3i\omega\nu_z\Gamma_n - 2v_{Fn}^2 k_z^2 & 2v_{Fn}^2 k_x k_z \\ 2v_{Fn}^2 k_x k_z & 3i\omega\nu_x/\Gamma_n - 2v_{Fn}^2 k_x^2 \end{pmatrix} \mathbf{E} \equiv -i\omega\hat{\chi}_n \mathbf{E}. \quad (11)$$

Here $\omega_{pn}^2 = 4\pi e^2 n_{0n}/m$ is the plasma frequency, $v_{Fn} = (\varepsilon_F/m)^{1/2}$ is the Fermi velocity, both related to normal electrons, $\Delta = 3i\omega\nu_x\nu_z - 2\nu_x\Gamma_n^{-1}v_{Fn}^2 k_z^2 - 2\nu_z\Gamma_n v_{Fn}^2 k_x^2$. Without spatial dispersion of normal electrons, i. e. at $v_{Fn} = 0$, this equation became the simple anisotropic Ohm law

$$\mathbf{j}_n = \hat{\sigma} \mathbf{E}, \quad \hat{\sigma} = \text{diag}(\sigma_{xx}, \sigma_{zz}), \quad (12)$$

where $\sigma_{xx} = \omega_{pn}^2 \Gamma_n / (4\pi\nu_x)$, $\sigma_{zz} = \omega_{pn}^2 / (4\pi\nu_z\Gamma_n)$ are respectively the in-plane and interlayer normal conductivities. Here it is worth to mention that such local model of normal conductivity has been used in works¹⁵⁻¹⁷ devoted to study the influence of the in-plane normal conductivity to the dynamics and stability of moving JVLs in layered HTSCs. Our approach naturally introduces into consideration the spatial dispersion originated from nonzero pressure of normal electrons.

C. Phonon contribution

This subsection is devoted to accounting for phonons in our phenomenological model describing Josephson dynamics of layered HTSCs. In the present paper we take into account only the direct excitation of infrared-active phonons by the electric field of Josephson oscillations. In fact here we will actually generalize the approach used in Refs. 18,19 to the case of non-uniform solutions in distributed Josephson systems. The nonlinear interaction between Josephson oscillations and phonons due to effects of phonon assisted tunneling considered in Refs. 20,21 would not be considered in this subsection, but later, when we formulate general nonlinear equation, we will show how this mechanism can be introduced in our model.

In order to find the phonon contribution to the dielectric permittivity we use standard approach (see, for example, Ref.22). Let us write the classical equation of motion for ions derived in Born-Oppenheimer adiabatic approximation,

$$M_\nu \ddot{\mathbf{z}}_N^\nu = - \sum_{\mu, \mathbf{M}} \hat{G}_{\mathbf{N}-\mathbf{M}}^{\nu\mu} \mathbf{z}_M^\mu + q_\nu \mathbf{E}_N^\nu. \quad (13)$$

In this formula \mathbf{z}_N^ν is the ion displacement from the equilibrium position, ν is the ion index in the unit cell, $\mathbf{N} = n_1 \mathbf{a}_1 + n_2 \mathbf{a}_2 + n_3 \mathbf{a}_3$ is the unit cell index, $\mathbf{a}_{1,2,3}$ are lattice periods, $\hat{G}_{\mathbf{N}-\mathbf{M}}^{\nu\mu}$ is the "seed" force tensor resulting from the interaction between ions via valence electrons, q_ν is the ion charge, M_ν is the ion mass, \mathbf{E}_N^ν is the microscopic electric field at the point of the ion. The interaction between ions and conductivity electrons is carried out via the last term in the r. h. s. of (13). In the equation (13) and further the product of a tensor and a vector is written in components as $(\hat{A}\mathbf{x})_i = A_{ij}x_j$. The relation between microscopic field and average macroscopic field can be written via so called Lorentz tensor $\hat{L}_{\mathbf{N}-\mathbf{M}}^{\nu\mu}$

$$\mathbf{E}_N^\nu = \mathbf{E}_N + 4\pi \sum_{\mu, \mathbf{M}} \hat{L}_{\mathbf{N}-\mathbf{M}}^{\nu\mu} \mathbf{P}_M^\mu, \quad (14)$$

where $\mathbf{P}_M^\mu = q_\mu \mathbf{z}_M^\mu$ is the dipole momentum of the μ -th ion in the \mathbf{M} -th cell. With the account for the difference between microscopic electric field from macroscopic field the equation for ν -th ion motion takes the form

$$M_\nu \ddot{\mathbf{z}}_N^\nu = - \sum_{\mu, \mathbf{M}} \hat{F}_{\mathbf{N}-\mathbf{M}}^{\nu\mu} \mathbf{z}_M^\mu + q_\nu \mathbf{E}_N, \quad (15)$$

where $\hat{F}_{\mathbf{N}-\mathbf{M}}^{\nu\mu} = \hat{G}_{\mathbf{N}-\mathbf{M}}^{\nu\mu} - 4\pi q_\nu \hat{L}_{\mathbf{N}-\mathbf{M}}^{\nu\mu} q_\mu$ is renormalized force tensor.

The contribution of ions into dielectric permittivity ε may be found from the expression for ion current density

$$\mathbf{j}_N = \frac{1}{V} \sum_{\nu} q_\nu \dot{\mathbf{z}}_N^\nu, \quad (16)$$

where V is the unit cell volume. After some algebra we get the ion current density

$$\mathbf{j}_i = -\frac{i\omega}{V} \sum_{a=1}^{3L} \frac{1}{-\omega^2 + \omega_{ph}^2(\mathbf{k}, a)} \frac{\sum_{\nu,\mu} q_\nu q_\mu \mathbf{e}_\nu(\mathbf{e}_\mu^*, \mathbf{E})}{\sum_\nu M_\nu \mathbf{e}_\nu^* \mathbf{e}_\nu} \equiv -i\omega \hat{\chi}_i \mathbf{E}, \quad (17)$$

where a is the phonon mode index, L is the number of ions in the unit cell, $\omega_{ph}(\mathbf{k}, a)$ is the phonon frequency, $\mathbf{e}_\nu(\mathbf{k}, a)$ is the polarization vector. $\omega_{ph}(\mathbf{k}, a)$ and $\mathbf{e}_\nu(\mathbf{k}, a)$ are yielded from the equation for eigenvalues and eigenvectors for the matrix $\hat{F}^{\nu\mu}(\mathbf{k})$

$$\sum_\mu \hat{F}^{\nu\mu}(\mathbf{k}) \mathbf{e}_\mu(\mathbf{k}, a) = M_\nu \omega_{ph}^2(\mathbf{k}, a) \mathbf{e}_\nu(\mathbf{k}, a), \quad (18)$$

where $\hat{F}^{\nu\mu}(\mathbf{k})$ is the Fourier image of the tensor $\hat{F}_{\mathbf{N}-\mathbf{M}}^{\nu\mu}$

$$\hat{F}^{\nu\mu}(\mathbf{k}) = \sum_{\mathbf{N}} e^{-i\mathbf{k}\mathbf{N}} \hat{F}_{\mathbf{N}}^{\nu\mu}. \quad (19)$$

The expression (17) is the well-known formula describing phonon contribution to dielectric permittivity, which may be found in many solid state physics courses. Of course, the concrete definition of phonon frequencies and polarization vectors for layered superconductors require detailed spectroscopic or numerical investigation. Example of calculations of phonon properties of typical layered superconductor with intrinsic Josephson effect $\text{Bi}_2\text{Sr}_2\text{CaCu}_2\text{O}_8$ can be found in Ref. 23.

So now we have found the contributions from normal electrons and phonons to the dielectric permittivities and are able to define electric displacement vector $\mathbf{D} = (\hat{I} + 4\pi\hat{\chi}_n + 4\pi\hat{\chi}_i)\mathbf{E} \equiv \hat{\varepsilon}\mathbf{E}$, using expressions (11) and (17) for susceptibilities $\hat{\chi}_n$ and $\hat{\chi}_i$.

The Eqs. (4a), (4b), (8a), (8b) together with the relations (11) and (17) represent complete system describing, in principle, all linear waves in long wavelength limit. However, this system does not describe Josephson vortex degree of freedom in layered HTSCs because it is linear and does not allow the finite jumps of the phase of order parameter. In the next subsection we will show how Josephson vortices can be included in the model and formulate general nonlinear model describing both Josephson vortex dynamics and linear waves in layered HTSCs. We will compare this model with several known ones, and reveal the relations between the parameters of continual model and the parameters of layered superconductors.

D. Discretization of the model

The aim of the present subsection is the transformation of the set of equations in the continual limit, to the form admitting solutions in the form of vortices, which are able to move along the layers of the HTSC. To do this, we split the continuous medium into the series of layers of thickness s equal to the period of the layers of the HTSC, and oriented perpendicular to the c axis of superconductor. We introduce new variables describing the corresponding fields at the moment t , coordinate x , and in some point within the n -th layer. It is possible provided field distributions are smooth inside the layer. After such discretization we allow the phase of order parameter to make a finite jump between layers and restore the nonlinear expression for the interlayer Josephson current.

First of all, let us decompose all dynamical variables to two sets defined on two different lattices shifted with respect to each other. The nodes of these two lattices can be thought to be placed in the middle of superconducting and dielectric layers, respectively. The nodes of these sublattices we will denote by the number of period n . We attribute the variables $E_x, D_x, j_x^{n,s,i}, v_x^{n,s,i}$ to the first set and $E_z, D_z, j_z^{n,s,i}, v_z^{n,s,i}$ to the second one. After such a decomposition we replace the derivatives of the dynamical variables over the coordinate perpendicular to the layers in the set of Eqs. (4a), (4b), (8a), (8b), (11), (17), by finite differences, using the following rule :

$$s \frac{\partial V}{\partial z} \rightarrow \pm V_{n\pm 1} \mp V_n, \quad s^2 \frac{\partial^2 V}{\partial z^2} \rightarrow V_{n+1} - 2V_n + V_{n-1} \equiv \Delta_n V_n, \quad (20)$$

where V_n stands for the one of the dynamical variables of the problem, upper sign should be used for variables from the first set and lower sign — for the second one. Such a rule of discretisation follows from integral form of Maxwell and hydrodynamic equations and provides necessary symmetry of finite-difference equations. To demonstrate how this procedure works let us apply it to well known telegraph equations describing electromagnetic waves in transmission lines

$$L\dot{I} + U_x = 0, \quad C\dot{U} + I_x = 0, \quad (21)$$

here U, I are voltage and current in the line, L, C are linear densities of inductance and capacity, respectively. Attributing voltage and current to different sets and replacing spatial derivatives by finite differences using our rule we come to equations

$$sL\dot{I}_n + U_n - U_{n-1} = 0, \quad sC\dot{U}_n + I_{n+1} - I_n = 0, \quad (22)$$

expressing two Kirchhoff laws for discrete L, C chain. Now let us return to our problem. Applying the formulated procedure to our set of differential the substitution (20) we obtain the following system

$$\frac{1}{c} \frac{\partial}{\partial t} E_{xn} = \frac{c}{2es} \frac{\partial}{\partial x} (p_{zn} - p_{zn-1}) - \frac{c}{2es^2} \Delta_n p_{xn} - \frac{4\pi}{c} \left(-\frac{en_0\Gamma_s}{2m} p_{xn} + j_{xn}^n + j_{xn}^i \right), \quad (23)$$

$$\frac{1}{c} \frac{\partial}{\partial t} E_{zn} = -\frac{c}{2e} \frac{\partial^2}{\partial x^2} p_{zn} - \frac{c}{2es} \frac{\partial}{\partial x} (p_{xn+1} - p_{xn}) + \frac{4\pi}{c} \left(-\frac{en_0}{2m\Gamma_s} p_{zn} + j_{zn}^n + j_{zn}^i - j_{ext} \right), \quad (24)$$

$$-\frac{1}{2e} \frac{\partial}{\partial t} p_{xn} = E_{xn} - r_d^2 \left(\frac{\partial^2}{\partial x^2} D_{xn} + \frac{1}{s} \frac{\partial}{\partial x} (D_{zn} - D_{zn-1}) \right), \quad (25)$$

$$-\frac{1}{2e} \frac{\partial}{\partial t} p_{zn} = E_{zn} - r_d^2 \left(\frac{1}{s} \frac{\partial}{\partial x} (D_{xn+1} - D_{xn}) + \frac{1}{s^2} \Delta_n D_{zn} \right), \quad (26)$$

$$\mathbf{D} = \hat{\varepsilon} \mathbf{E}, \quad \mathbf{j}^{n,i} = \frac{\partial}{\partial t} (\hat{\chi}_{n,i} \mathbf{E}), \quad \hat{\varepsilon} = \hat{I} + 4\pi \hat{\chi}_n + 4\pi \hat{\chi}_i. \quad (27)$$

The Eq. (27) of this system combines the contributions from normal electrons and phonons which are given by the formulas (11) and (17) for corresponding tensors of susceptibilities. In a common case, when spacial dispersion takes place, these tensors contain wavevectors in the interlayer direction. Therefore, the procedure of discretization should be applied also to Eq. (27) accounting for specific expressions for normal electron and phonon contributions to dielectric permittivity.

Now this system allows finite jumps of physical variables but it still remains linear and, therefore, does not describe Josephson vortices. To describe them we need to introduce Josephson nonlinearity in the expression for interlayer supercurrent. This procedure is made in the following way. Integrating the expression for z -component of the superconducting momentum over z from n -th to $n+1$ -th layer, we get Josephson phase difference

$$\theta_n = -\frac{1}{\hbar} \int_{ns + \frac{ds}{2}}^{(n+1)s + \frac{ds}{2}} p_z dz = \chi_n - \chi_{n+1} - \frac{2\pi}{\Phi_0} \int_{ns + \frac{ds}{2}}^{(n+1)s + \frac{ds}{2}} A_z dz. \quad (28)$$

Then we need to substitute θ_n into the set of equations in a correct way. As the interlayer supercurrent in layered HTSCs has Josephson nature, we need to substitute $p_{zn} \rightarrow -\hbar s^{-1} \sin \theta_n$ in the last term of the Eq. (24). The remaining terms in Eqs. (23) and (24) having p_{zn} are in fact the components of $[\nabla, \mathbf{B}]$, that is why in these terms $p_{zn} \rightarrow -\hbar s^{-1} \theta_n$. The Eq. (26) at $r_d = 0$ is actually the Josephson relation $\hbar \dot{\theta} = 2eU$, then in this expression also $p_{zn} \rightarrow -\hbar s^{-1} \theta_n$. At $r_d \neq 0$ the Eq. (26) describes violation of the Josephson relation due to charge effects; the influence of these effects on Josephson dynamics is considered later, in the section devoted to numerical experiment.

Let us rewrite the system (23), (24), (25), (26), (27) in the notations used when describing bulk superconductors:

$$j_c = \frac{\Phi_0}{8\pi^2 cs} \frac{\omega_{ps}^2}{\Gamma_s}, \quad \lambda_{ab}^2 = \frac{c\Phi_0}{8\pi^2 j_c s \Gamma_s^2} = \frac{c^2}{\Gamma_s \omega_{ps}^2}, \quad r_d^2 = \frac{v_{Fs}^2}{\omega_{ps}^2} \frac{ds}{s}.$$

As a result, we get the following set of equations:

$$\frac{1}{c} \frac{\partial}{\partial t} E_{xn} = -\frac{\Phi_0}{2\pi s^2} \frac{\partial}{\partial x} (\theta_n - \theta_{n-1}) + \frac{4\pi}{c} \frac{\lambda_{ab}^2}{s^2} \Delta_n j_{xn}^s - \frac{4\pi}{c} (j_{xn}^s + j_{xn}^n + j_{xn}^i), \quad (29)$$

$$\frac{1}{c} \frac{\partial}{\partial t} E_{zn} = \frac{\Phi_0}{2\pi s} \frac{\partial^2}{\partial x^2} \theta_n - \frac{4\pi \lambda_{ab}^2}{cs} \frac{\partial}{\partial x} (j_{xn+1}^s - j_{xn}^s) - \frac{4\pi}{c} (j_c \sin \theta_n + j_{zn}^n + j_{zn}^i - j_{ext}), \quad (30)$$

$$\frac{4\pi \lambda_{ab}^2}{c^2} \frac{\partial}{\partial t} j_{xn}^s = E_{xn} - \frac{sr_d^2}{ds} \left(\frac{\partial^2}{\partial x^2} D_{xn} + \frac{1}{s} \frac{\partial}{\partial x} (D_{zn} - D_{zn-1}) \right), \quad (31)$$

$$\frac{\Phi_0}{2\pi cs} \frac{\partial}{\partial t} \theta_n = E_{zn} - \frac{sr_d^2}{ds} \left(\frac{1}{s} \frac{\partial}{\partial x} (D_{xn+1} - D_{xn}) + \frac{1}{s^2} \Delta_n D_{zn} \right). \quad (32)$$

$$\mathbf{D} = \hat{\varepsilon} \mathbf{E}, \quad \mathbf{j}^{n,i} = \frac{\partial}{\partial t} (\hat{\chi}_{n,i} \mathbf{E}), \quad \hat{\varepsilon} = \hat{I} + 4\pi \hat{\chi}_n + 4\pi \hat{\chi}_i. \quad (33)$$

The model represented by these equations (29), (30), (31), (32), (33) describes interaction of Josephson vortices with electromagnetic waves, plasmons, and phonons on an equal footing. This model possesses the necessary symmetry with respect to permutation of x, z coordinates and describes the spatial dispersion resulted from electron and ion degree of freedom in the system. Besides, our system allows to account for the influence of linear modes of any nature to the dynamics of Josephson vortices in a layered HTSC, by inclusion of the corresponding terms into the dielectric permittivity $\hat{\epsilon}$. Say, in recently discovered FeAs based superconductors^{24–26} it can turn out that magnetic degrees of freedom play an important role. Our approach allows to include them in this general scheme.

Of course, our general model contain the particular theories considered in earlier works as a limiting cases. Among these special cases are the model with the magnetic coupling between the layers^{5,6}, the model with the charge coupling between the layers⁷, the model taking into account the in-plane quasiparticle current¹⁵, the model accounting for the infrared-active phonons polarized perpendicular to the layers^{18,19}, etc. Results of two works^{8,9}, where the attempt to unify magnetic and charge coupling have been undertaken also can be reproduced by our model. But our model have extra terms in Eqs. (31) and (32) containing $\partial/\partial x$ which are absent in Refs 8,9. Although small far from resonances, these terms become significant when Josephson frequency get close to phonon and plasmon frequencies.

The set of Eqs. (29), (30), (31), (32), (33) contains the only nonlinear term, which describes Josephson nonlinearity. While deriving this system we have neglected all hydrodynamic nonlinearities such as nonlinear dependence of a pressure on concentration, difference between Lagrange and Euler variables, nonlinear expression for the current density and so on. The account for these terms would lead to the existence of combination processes, such as, for example, Raman and Brillouin scattering. Due to strong anisotropy of the layered HTSCs, the most significant effects of this type are the ones providing the dependence on concentration of the parameters determining the transport and elastic properties of the material in the direction of c -axis, such as Josephson critical current density j_c , interlayer normal conductivity σ_{zz} , etc. The accounting for these dependencies leads to such effects as phonon-assisted tunneling due to the interaction of the electrons with Raman-active phonons. This effect has been considered in Ref. 21 for acoustic phonons in long Josephson junction and later in Ref. 20 for intrinsic junctions. The similar effect should be also expected for plasmons. In the present work we restrict ourselves to the case when these effects are unimportant.

Let us consider now the examples how some known models arise from our equations in the limiting cases. For instance, if we set the phonon current, the in-plane displacement and normal currents to be equal to zero ($j_{x,z,ph} = \partial E_{xn}/\partial t = j_{xn}^n = 0$), propose the interlayer normal current to have the purely Ohmic character ($j_{zn} = \sigma_{zz} E_{zn}$), and neglect the nonzero screening length of the longitudinal electric field ($r_d = 0$), we obtain

$$\frac{\partial^2 \theta_n}{\partial x^2} = \left(\frac{1}{\lambda_j^2} \Delta_n + \frac{1}{\lambda_c^2} \right) \left(\omega_j^2 \frac{\partial^2 \theta_n}{\partial t^2} + \sigma_{zz} \frac{\Phi_0}{2\pi cs} \frac{\partial \theta_n}{\partial t} + \sin \theta_n - \frac{j_{ext}}{j_c} \right), \quad (34)$$

where $\lambda_j = \Gamma_s s$, $\lambda_c = \Gamma_s \lambda_{ab}$, $\omega_j^2 = (8\pi^2 j_c cs)/\Phi_0$. First this set of equations has been derived in Refs. 5,6 and describes the Josephson dynamics of stacked distributed Josephson junctions and layered superconductors with the magnetic coupling between the layers. In another case, when we suppose the lateral dimensions of the system to be smaller than Josephson length, so that $\partial/\partial x = 0$, neglect phonons, and set $j_{zn} = \sigma_{zz} E_{zn}$, we obtain

$$\frac{1}{c^2} \frac{\partial^2 \theta_n}{\partial t^2} = -\frac{1}{\lambda_c^2} (1 - \eta \Delta_n) \left(\sin \theta_n - \frac{j_{ext}}{j_c} \right) - \frac{4\pi \sigma_{zz}}{c^2} \frac{\partial \theta_n}{\partial t}, \quad (35)$$

where $\eta = r_d^2/(sd_s)$ is the parameter of charge coupling. This set of equations has been first considered in Ref. 7 and describes the dynamics of the layered superconductor with the charge coupling between the layers. Other particular examples of models considered earlier may be obtained from our model in a similar way.

III. DISPERSION CHARACTERISTICS OF LINEAR WAVES.

The layered HTSCs has a wide spectrum of eigenwaves which, in principle, may be radiated by a moving JVL. The linear modes excited by JVL, in turn, may affect the shape and mutual arrangement of vortices in the lattice. The excitation of linear waves by the moving JVL leads to appearance of resonant steps on CVCs with the frequencies being equal to the ones of the radiated modes. In order to identify the resonances on CVC it is necessary to know the dispersion characteristics of linear waves in layered HTSCs, which can give much information about eigenmodes in the material and conditions of their excitation.

In order to build the dispersion characteristics we first linearize the set of Eqs. (29), (30), (31), (32), (33) assuming $|\theta_n| \ll 1$, so that $\sin \theta_n \approx \theta_n$, and set the bias current to zero. We also neglect dissipation in the system ($\sigma_{xx} = \sigma_{zz} = 0$) keeping in mind that it may be accounted for by perturbation theory. Taking all dynamic variables

$\sim \exp(ikx + iqy - i\omega t)$ and setting the determinant of the obtained linear system to zero, we get the dispersion equation of the linear modes. It has the standard form

$$\det \left\| \frac{\omega^2}{c^2} \varepsilon_{totalij}(\omega, \mathbf{k}) + k_i k_j - k^2 \delta_{ij} \right\| = 0, \quad (36)$$

where $\hat{\varepsilon}_{total}$ contains linear contributions from superconducting and normal electrons, and phonons. For short, we do not write this equation in an explicit form. We also assume the simple model expression of phonon susceptibility

$$\hat{\chi}_{ph} = -\frac{1}{4\pi} \begin{pmatrix} \frac{\Omega_x^2}{\omega^2 + i\omega\gamma_{ph_x} - \omega_{0x}^2} & 0 \\ 0 & \frac{\Omega_z^2}{\omega^2 + i\omega\gamma_{ph_z} - \omega_{0z}^2} \end{pmatrix}. \quad (37)$$

This expression describes two optical phonon modes: one polarized along the layers (x -phonon) and other polarized perpendicular to the layers (z -phonon). Here ω_{0x} and ω_{0z} are the frequencies of the x -phonon and the z -phonon, respectively, γ_{ph_x} and γ_{ph_z} the damping coefficients of these modes, Ω_x and Ω_z are the oscillator strengths. For simplicity we assume $\omega_{0x,z}$, $\gamma_{ph_{x,z}}$, and $\Omega_{x,z}$ to be independent of the quasimomentum, i. e. the bare phonon modes has no spatial dispersion. Moreover, in this section we neglect phonon damping ($\gamma_{ph_{x,z}} = 0$), assuming that it may be accounted for by perturbation theory. We will return to the nonzero $\gamma_{ph_{x,z}}$ later, in numerical experiment.

In our previous work we have considered wave vector surfaces for the analysis of the dispersion characteristics of the layered superconductor with phonons in the continual limit²⁷. Now we build the dispersion curves $\omega(k, q)$ for the periodic system.

The dispersion curves of linear modes in a layered HTSC are schematically shown in Fig. 2. The electromagnetic, plasma, and phonon modes are shown. We build the dispersion characteristics for certain directions in the Brillouin zone. The curves in the right part of the plot are for the $\Gamma - X$ direction (growing k), the curves in the central part of the plot are for the $\Gamma - X$ direction (growing q), and the curves in the left part are for the $X - W$ direction (growing k), along the edge of the Brillouin zone. We use standard notations Γ, X, W for the points of the Brillouin zone. The dispersion curves for the case of absence of the interaction between electromagnetic and plasma modes with phonons, i. e. at zero oscillator strengths ($\Omega_{x,z} = 0$), are plotted by dashed lines. It is seen that at nonzero oscillator strengths the splitting of dispersion curves appears in the places of intersection between bare curves.

We note that due to anisotropy the separation of modes into the electromagnetic and plasma mode is relative, depending on the direction of the wave. For example, consider the lowest branch of the dispersion characteristics. The wave having $q = 0$ is the electromagnetic mode and the one having $k = 0$ is the plasma mode. And vice versa, for highest branch, the wave with $q = 0$ is the plasma mode and the one with $k = 0$ is the electromagnetic mode. For the arbitrary direction of the wave vector is it impossible to say whether it is an electromagnetic or plasma wave.

The frequency of the lowest branch of the dispersion characteristics corresponding to the point Γ ($k = 0, q = 0$) is ω_j —the frequency of the Josephson plasma resonance. In the notations of the hydrodynamic model it is equal to $\omega_{ps}/\sqrt{\Gamma_s}$. The typical values of ω_j for layered HTSCs are of the order 100 GHz. At the values of the parameters corresponding to layered HTSCs, the frequencies of the highest branch of the dispersion characteristics are in the optical range. Therefore, this mode cannot affect the JVL motion in the layered superconductors.

The important particular case of the modes in a layered HTSC is the Swihart wave, i. e. the mode belonging to the lowest branch of the dispersion characteristics, which propagating along the layers and having the standing wave structure in the direction perpendicular to the layers. The dispersion curve $\omega(k)$ of this wave has the form of the hyperbole. The slope of the asymptotes of this curve determines the Swihart velocity

$$\bar{c}^2(q) = \mu \frac{\varepsilon_{zz}^{-1} + 2\eta(1 - \cos q)}{1 + 2\mu(1 - \cos q)}, \quad (38)$$

where q is the transverse wave number of the Swihart wave. It is seen that the antisymmetric ($q = \pi$) Swihart mode is the slowest one, and the symmetric ($q = 0$) mode is the fastest one. We will use the formula (38) for the analyzing the results of the numerical experiment.

IV. NUMERICAL EXPERIMENT

Now we apply the derived system (29), (30), (31), (32), (33) to the numerical investigation of the dynamics of Josephson vortices in layered superconductors with the account for their interaction with various linear modes. The motion of Josephson vortex lattice (JVL) leads to excitation of linear modes of a layered HTSC which, generally, affect

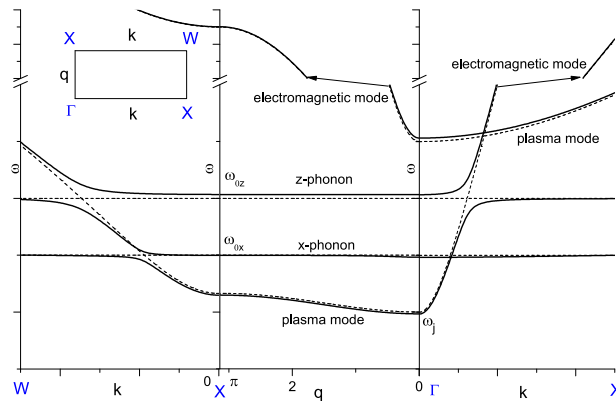


FIG. 2: (Color online) The schematic drawing of the dispersion characteristics of linear waves in a layered HTSC. The dashed lines show the dispersion without the interaction with phonon modes. The inset shows the fragment of the Brillouin zone of the layered structure.

the moving lattice, leading to distortions in vortex shape and changes in their mutual arrangement. The excited linear modes may lead to resonances on CVCs of layered HTSCs with moving JVL. In the present section we numerically investigate the excitation of linear waves by the moving JVL, and their influence on CVCs, accounting for possible changes in vortex shape and their rearrangement.

In the numerical experiment we use periodic boundary conditions in both in-plane and interlayer directions for all variables. However, for Josephson phase difference θ_n the boundary conditions in x -direction is modified so that

$$\theta_n(L) = \theta_n(0) + 2\pi R_n, \quad (39)$$

where R_n is the number of vortices trapped in the n -th junction of the stack, and L is the length of the system in the longitudinal direction. Instead of θ_n we introduce $\theta'_n = \theta_n - 2\pi R_n x/L$ satisfying the periodic boundary condition in the longitudinal direction. Accounting for this, we write the expression for the interlayer Josephson current as $j_c \sin(\theta'_n + 2\pi R_n x/L)$. The choice of boundary conditions described above provides the simplicity of numerical solution of the system; however, when using such conditions one takes into account only volume effects, neglecting the influence of boundaries on Josephson vortex dynamics.

In order to solve the system (29), (30), (31), (32), (33) numerically we transform it to the set of evolutionary equations in ordinary derivatives in time. To do this, we use the exponential Fourier transform by standard 2D-FFT algorithm. The obtained set of ordinary time-dependent differential equations is solved by Krank-Nikolson scheme. The similar approach to the numerical experiment has been used in Ref. 10.

The periodic boundary conditions along the layers imply that the number of vortices captured in each junction of the system is a constant. In our calculation we assume the number of vortices to be the same for all layers and denote it as R .

In the numerical experiment we use the typical values of the parameters of $\text{Bi}_2\text{Sr}_2\text{CaCu}_2\text{O}_8$: $j_c = 150 \text{ A/cm}^2$, $\lambda_{ab} = 1700 \text{ \AA}$, $s = 15 \text{ \AA}$, $\sigma_{ab} = 5 \cdot 10^4 (\Omega \cdot \text{cm})^{-1}$, $\sigma_c = 2 \cdot 10^{-3} (\Omega \cdot \text{cm})^{-1}$, $\varepsilon_{zz} = 12$. The parameters of phonons have been taken from the experimental data obtained by spectral ellipsometry²⁸. In the following we assume the length of the system L to be measured in the units of Josephson length $\lambda_j = \Gamma_s s$ and the bias current density to be measured in the units of Josephson critical current j_c . In the calculations we use values of L corresponding to the ones of the patterns used in experiments. The number of vortices in a layer is set so that it corresponds to the dense JVL (at a given L). We also assume the frequencies and the voltages to be measured in the units of $\omega_p \Gamma_s^{-1/2}$.

A. Results

This subsection is devoted to the results of the numerical modeling of the dynamics of the JVL in a layered HTSC performed basing on the derived model. First, we investigate the simplest case, when the spatial dispersion, phonons, and all interlayer couplings except the magnetic one are neglected. Then, we complicate the problem step-by-step, introducing phonon susceptibility, charge coupling, and study the effects caused by these complications.

1. *The simplest case—the magnetic coupling without phonons and spatial dispersion.*

To check the efficiency of the used numerical scheme we perform the calculation of the CVC of the layered HTSC with the moving JVL in the case of absence of spatial dispersion, phonons, and in-plane dissipation. The interlayer normal current is assumed to be purely ohmic. This approximation corresponds to the case of magnetic coupling between the layers, which has been considered in Refs. 5,6.

Consider the CVC built for the case $R = 6$ which corresponds to typical values of the external magnetic field (Fig. 3). At $j_{ext} = 0$ a triangular JVL is established in the structure (Fig. 4). As the bias current increases, the JVL moves with the increasing velocity, keeping the triangular vortex arrangement. When the bias current reaches 0.18, the JVL velocity stops growing, so that the voltage on the structure is established at the value 0.18. This step denoted by 1 appears due to coincidence of the JVL velocity with the characteristic velocity of the antisymmetric ($q = \pi$) Swihart mode of a layered HTSC.

The JVL remains triangular on the whole step 1; the vortex shape exhibit specific distortions due to the resonant increase of the harmonics with $q = \pi$ which grow as the bias current increases. The distribution of the magnetic field in this regime does not qualitatively differ from the static one (Fig. 4).

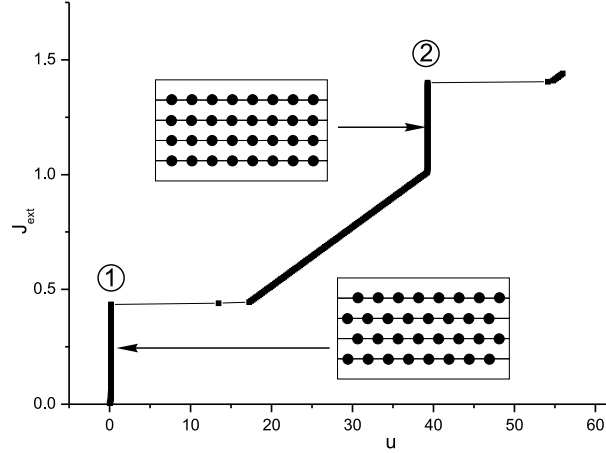


FIG. 3: A CVC of the layered HTSC with the moving JVL. The digits enumerate the steps of the CVC in the order of resonance frequencies increase. The insets schematically show the mutual arrangement of vortices on different resonance steps.

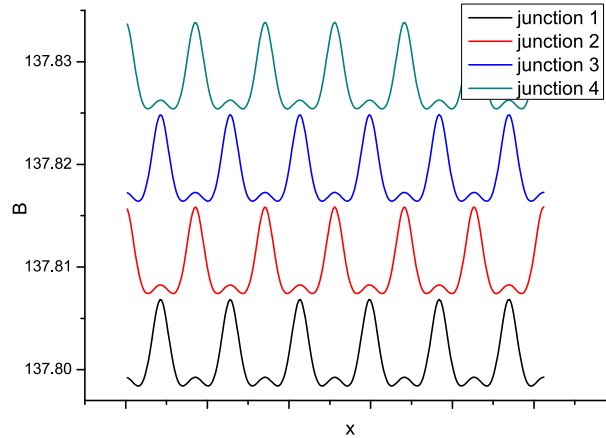


FIG. 4: (Color online) The magnetic field distribution corresponding to the static vortex lattice ($j_{ext} = 0$). For the sake of convenience, here and in the subsequent figures we add constants to the distributions of the magnetic field in different junctions. The actual value of the constant component of the magnetic field is as for the junction 1.

At the value $j_{ext} = 0.44$ the CVC jumps from the step 1 to the Ohmic branch. The amplitude of the electromagnetic field on the Ohmic branch is small and the vortices form rectangular lattice.

When the bias current reaches the value $j_{ext} \approx 1.0$ the second step on the CVC appears. This step is due to the resonance with the symmetric ($q = 0$) Swihart mode. In this regime, the moving vortices still form the rectangular

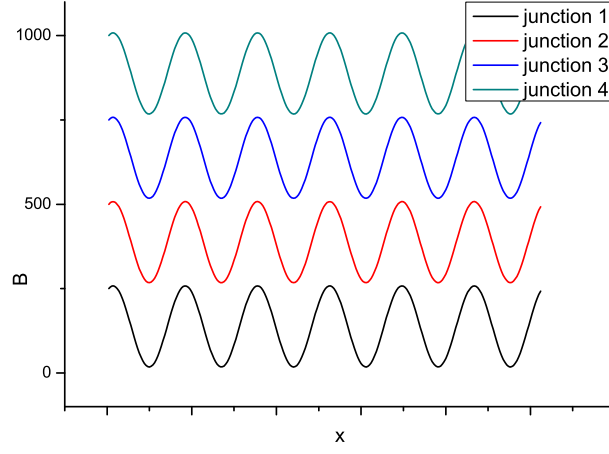


FIG. 5: (Color online) The magnetic field distribution corresponding to the end of the step 2 in Fig. 3. Here $j_{ext} = 1.4$. Giant amplitude of the electromagnetic field.

lattice, but the amplitude of the electromagnetic field sharply increases. This regime of vortex motion is characterized by large amplitude of the electromagnetic wave which accompanies the moving JVL, the amplitude of the wave grows with the bias current increase (Fig. 5).

With further bias current increase the CVC again jumps to the Ohmic branch. The magnetic field distribution in this regime does not qualitatively differ from the one between the steps 1 and 2.

The CVC obtained in our calculations is similar to the one obtained for two-stacked long Josephson junctions²⁹. The only difference is that in our CVC the voltages of the steps differ by two orders from each other. This is due to the fact that the magnetic coupling in layered HTSCs is usually much stronger than the one of artificial multilayer structures.

Consider now the CVC of the layered HTSC with the moving JVL at smaller external magnetic field ($R = 4$) (Fig. 6). One can see that, in addition to steps 1 and 3 corresponding to the resonances with the antisymmetric Swihart mode ($u = 0.14$) and the symmetric Swihart mode ($u = 32$), respectively, there is a step 2 corresponding to half a frequency of the resonance with the symmetric Swihart mode. The magnetic field distribution on this step is shown in Fig. 7. It is seen that there are two oscillations of the magnetic field per spatial period of the system, though four magnetic flux quanta are captured in each junction of the stack. This regime also shows a large amplitude of the electromagnetic field. The distributions of the magnetic field and the mutual arrangement of vortices at the steps 1 and 3 and between the resonances are similar to the ones for the case considered earlier (see Figs. 3, 4, 5).

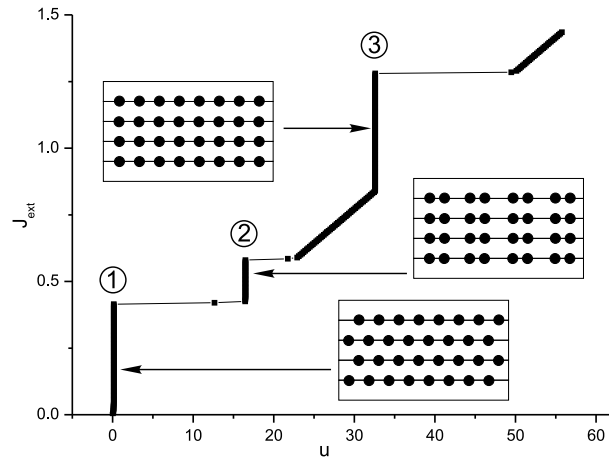


FIG. 6: CVC of the layered HTSC with moving JVL for weaker external magnetic field.

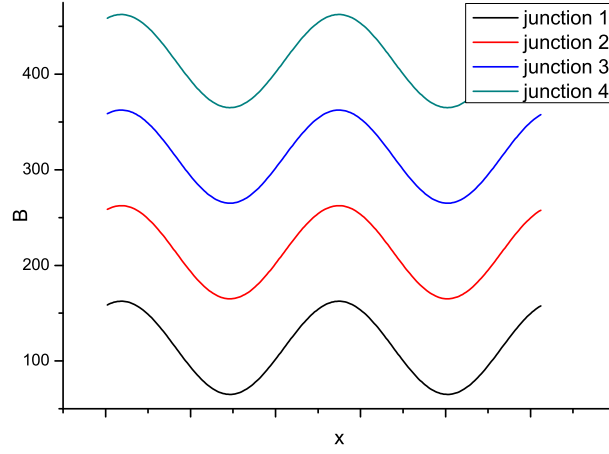


FIG. 7: (Color online) The magnetic field distribution corresponding to the end of the step 2 in Fig. 6. Here $j_{ext} = 0.58$.

2. Excitation of a phonon by moving vortex lattice.

The complex chemical composition of layered HTSCs provide large amount of phonon modes in such materials. Among these modes, there are "soft" phonons having frequencies of the order of several THz, which are smaller than the frequency of the energy gap in HTSCs. This makes possible the excitation of such phonon modes by a JVL moving in a layered HTSC. In this subsection we investigate the phonon excitation by a moving JVL.

For the calculations we slightly complicate the model used in the previous subsection, introducing the simplified expression (37) for the phonon susceptibility. The phonon parameters used in calculations are taken from Ref. 28.

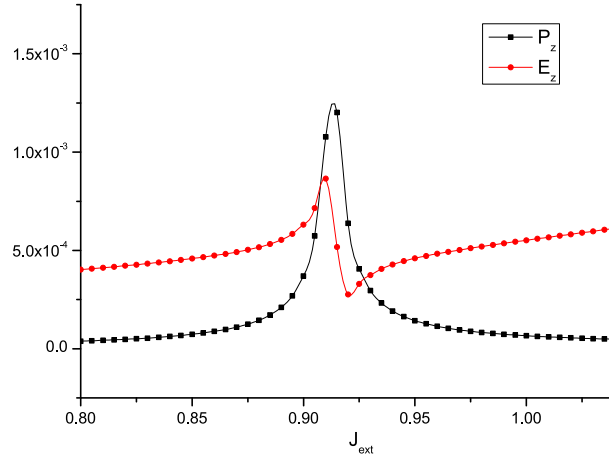


FIG. 8: (Color online) The amplitudes of alternate components of the electric field and the polarization vs. external current in the vicinity of the phonon frequency.

The Figs. 8 and 9 illustrate the excitation of the phonon z -phonon by the moving JVL. The Fig. 8 shows the dependence of complex amplitude modules of P_z and E_z harmonics with $q = 0$ and $k = k_{lattice}$, on the bias current. Here P_z is the z -component of the phonon polarization and $k_{lattice} = 2\pi RL^{-1}$ is the wavenumber of the main harmonic of the JVL. The peak on the dependence $P_z(j_{ext})$ is due to the excitation of the phonon mode and appears at the value of j_{ext} which corresponds to the JVL motion with the frequency of the phonon. The Fig. 9 shows the peak on the contribution to the CVC due to the extra energy needed to excite the phonon. The similar phonon peaks on the CVC has been obtained earlier^{18,19} for the case of spatially uniform Josephson junctions and junction chains. Our model actually generalizes the one used in Ref. 19 to the case of distributed Josephson junctions and junction stacks.

In the present simulations we do not consider the excitation of the x -phonons. The reason is that the JVL is rectangular at low enough external magnetic field and at the frequencies close to the phonon one. As one can see from the Eqs. (29), (30), (31), (32), x -phonon is not excited by a rectangular JVL, as $E_x = 0$ in such a lattice. However, if the tensor of phonon susceptibility contains non-diagonal components, the excitation of x -phonons by E_z of the

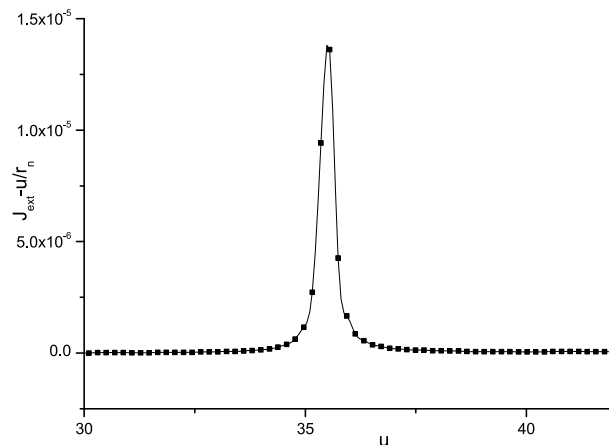


FIG. 9: Contribution to CVC due to excitation of the phonon mode in a HTSC.

moving rectangular JVL is possible.

In this subsection we have considered the excitation of a phonon by a moving JVL provided the condition that the phonon frequency is far from the frequencies of Swihart modes at a given $k_{lattice}$. The next subsection is devoted to the situation when the phonon frequency coincides with the frequency of one of the Swihart modes.

3. Excitation of the hybrid phonon+Swihart mode by a moving Josephson vortex lattice.

By choosing the external magnetic field applied to the structure, it is possible to make the frequency of the Swihart mode at $k = k_{lattice}$ equal to the phonon frequency. The Fig. 11 shows the contribution to the CVC in the vicinity of the bias current value corresponding to the phonon frequency. Two peaks located close to each other and having nearly equal height appear due to excitation of two modes with close frequencies. To explain this effect, consider the fragment of the dispersion characteristic of linear waves in a layered HTSC in the vicinity of the point where the Swihart mode and the phonon mode interact (Fig. 10). In the absence of the interaction the dispersion characteristic would have the shape shown by dotted line, here the slanted line shows the dispersion of the Swihart mode and the horizontal line shows the phonon dispersion.

In the presence of the interaction between two modes ($\Omega_x, \Omega_z \neq 0$) the dispersion characteristic takes the form shown by solid line in the Fig. 10. The magnitude of the dispersion curve splitting is determined by the oscillator strength of the phonon mode (Ω_x or Ω_z , depending on the polarization of the mode interacting with the Swihart wave). The intersection points of the vertical line corresponding to $k_{lattice}$, and dispersion curves, give the resonance frequencies.

The Fig. 11 shows the contribution to the CVC from the excited hybrid phonon+Swihart modes. The distance between two peaks is equal to the difference between the resonance frequencies obtained from the dispersion characteristic. We note that the height of the peaks in Fig. 11 is of two orders higher than the height of the peak caused by the excitation of the pure phonon mode (Fig. 9).

4. The violation of the Josephson relation — separation of normal electron charges by a moving JVL.

In this subsection we investigate the influence of the charge effects on the JVL motion in layered HTSCs. Starting again from the simple model with the magnetic coupling, we now assume the parameter of the charge coupling to be nonzero $\eta \neq 0$ and find out the differences in JVL dynamics compared to the case $\eta = 0$ considered above.

Consider CVC of the layered superconductor, calculated in the absence of phonons and in the presence of the charge coupling (Fig. 12, dashed line). As it is seen from this figure, there are two steps of this CVC. As in the absence of the charge coupling, they appear due to resonance with the antisymmetric and symmetric Swihart modes. Let us consider the differences between CVCs in Figs. 3 and 12. The first one is that the frequency of the first step is shifted towards higher frequencies, while the frequency of the second step is not changed. As in the case of zero charge coupling, the step positions correspond to the formula $\omega_{res} = \bar{c}(q)2\pi RL^{-1}$, where $\bar{c}(q)$ is determined by the expression (38).

The second feature of the regime with nonzero charge coupling is that the amplitude of the second step is much smaller than in the case of zero charge coupling. To explain this effect, consider the dependence of the Josephson

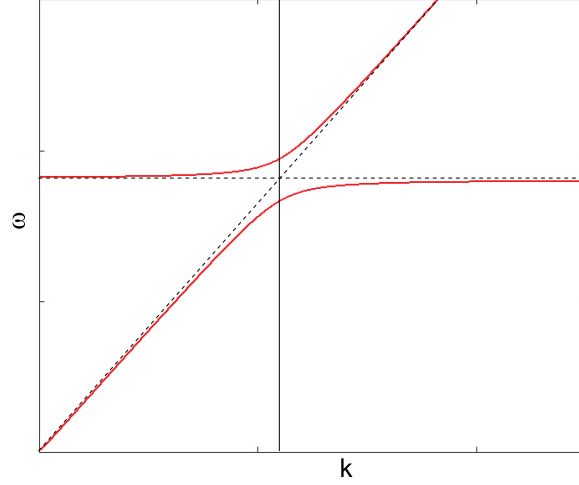


FIG. 10: (Color online) Dispersion characteristic of the symmetric Swihart mode and phonon mode in the vicinity of their interaction point.

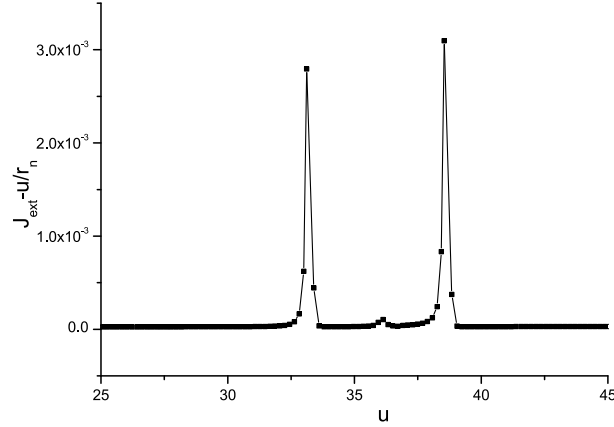


FIG. 11: Contribution to CVC due to the excitation of the hybrid phonon+Swihart modes.

phase growth rate on the bias current (Fig. 12, solid lines). It is seen that the phase growth rates vary from one junction to another or, the same, the vortex chains in different junction have different velocities. At the same time, the voltages on each junction are the same. According to the Eq. (32), this is the demonstration of the violation of the Josephson relation. As it is also seen from Fig. 12, only two or three junctions of possible four ones are locked to the second resonance of CVC. Therefore, the range of bias currents where the system remains on the resonant step, is smaller than in the case of zero charge coupling, when all junctions are locked.

V. CONCLUSION

We propose the comprehensive phenomenological model which describes the dynamics of the non-uniform distributions of Josephson phase difference in layered HTSCs, e. g. moving Josephson vortices and linear waves of any nature. Basing on this system we numerically build CVCs of a layered superconductor with the moving JVL and demonstrate the excitation of linear modes by moving vortices. The proposed model is shown to cover many effects which have been studied in previous works; in addition, we observe some new effects such as excitation of a phonon and hybrid modes by a moving JVL in layered superconductors.

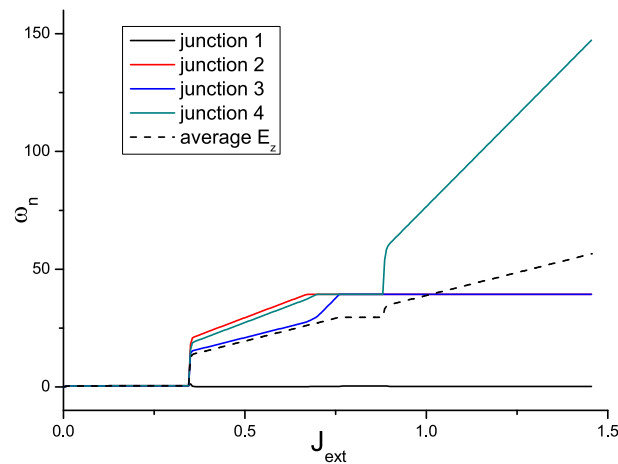


FIG. 12: (Color online) Dependence of phase growth rate in Josephson junctions of the structure, on the bias current. Dashed line shows the constant component of the electric field E_z in each junction.

VI. ACKNOWLEDGEMENTS

This work has been supported by the Russian Foundation for Basic Research (Grant # 09-02-01358-a), and by the following programs of the Russian Academy of Science: "Nonlinear Dynamics", "Quantum Macrophysics", and "Problems of Radiophysics".

* Electronic address: chig@ipm.sci-nnov.ru

- ¹ L. Ozyuzer, A. E. Koshelev, C. Kurter, N. Gopalsami, Q. Li, M. Tachiki, K. Kadowaki, T. Yamamoto, H. Minami, H. Yamaguchi, et al., *Science* **318**, 1291 (2007).
- ² R. V. Karlson and A. M. Goldman, *Phys. Rev. Lett.* **34**, 11 (1975).
- ³ Ya. G. Ponomarev, *Phys. Usp.* **45**, 649 (2002).
- ⁴ W. L. Mochán, M. del Castillo-Mussot, and R. G. Barrera, *Phys. Rev. B* **35**, 1088 (1987).
- ⁵ S. Sakai, P. Bodin, and N. F. Pedersen, *J. Appl. Phys.* **73**, 2411 (1993).
- ⁶ L. N. Bulaevskii, M. Zamora, D. Baeriswyl, H. Beck, and J. R. Clem, *Phys. Rev. B* **50**, 12831 (1994).
- ⁷ T. Koyama and M. Tachiki, *Phys. Rev. B* **54**, 16183 (1996).
- ⁸ Ju H. Kim and J. Pokharel, *Physica C* **384**, 425 (2003).
- ⁹ M. Machida and S. Sakai, *Phys. Rev. B* **70**, 144520 (2004).
- ¹⁰ A. V. Chiginev and V. V. Kurin, *Phys. Rev. B* **70**, 214523 (2004).
- ¹¹ D. A. Ryndyk, *JETP Lett.* **65**, 791 (1997).
- ¹² D. A. Ryndyk, *Phys. Rev. Lett.* **80**, 3376 (1998).
- ¹³ D. A. Ryndyk, *JETP* **89**, 975 (1999).
- ¹⁴ D. A. Ryndyk, V. I. Pozdnjakova, I. A. Shereshevskii, and N. K. Vdovicheva, *Phys. Rev. B* **64**, 052508 (2001).
- ¹⁵ A. E. Koshelev, *Phys. Rev. B* **62**, R3616 (2000).
- ¹⁶ A. E. Koshelev and I. S. Aranson, *Phys. Rev. Lett.* **85**, 3938 (2000).
- ¹⁷ A. E. Koshelev and I. Aranson, *Phys. Rev. B* **64**, 174508 (2001).
- ¹⁸ Ch. Helm, Ch. Preis, F. Forsthofer, J. Keller, K. Schlenga, R. Kleiner, and P. Müller, *Phys. Rev. Lett.* **79**, 737 (1997).
- ¹⁹ Ch. Helm, Ch. Preis, Ch. Walter, and J. Keller, *Phys. Rev. B* **62**, 6002 (2000).
- ²⁰ E. G. Maksimov, P. I. Arseyev, and N. S. Maslova, *Solid State Comm.* **111**, 391 (1999).
- ²¹ Yu. M. Ivanchenko and Yu. V. Medvedev, *Sov. Phys.-JETP* **33**, 1223 (1971).
- ²² J. M. Ziman, *Principles of the Theory of Solids* (Cambridge at the University Press, 1972).
- ²³ J. Prade, A. D. Kulkarni, F. W. de Wette, U. Schroeder, and W. Kress, *Phys. Rev. B* **39**, 2771 (1989).
- ²⁴ M. V. Sadovskii, *Phys. Usp.* **51**, 1201 (2008).
- ²⁵ A. L. Ivanovskii, *Phys. Usp.* **51**, 1229 (2008).
- ²⁶ Yu. A. Izyumov and E. Z. Kurmaev, *Phys. Usp.* **51**, 1261 (2008).
- ²⁷ A. V. Chiginev and V. V. Kurin, *Supercond. Sci. Tech.* **20**, S34 (2007).
- ²⁸ N. N. Kovaleva, A. V. Boris, T. Holden, C. Ulrich, B. Liang, C. T. Lin, C. Bernhard, J. L. Tallon, D. Munzar, and A. M. Stoneham, *Phys. Rev. B* **69**, 054511 (2004).
- ²⁹ A. Petraglia, A. V. Ustinov, N. F. Pedersen, and S. Sakai, *J. Appl. Phys.* **77**, 1171 (1995).